

## Direct Observation of Molecule-Substrate Antibonding States near the Fermi Level in Pd(110)- $c(4 \times 2)$ -Benzene

Jun Yoshinobu\* and Maki Kawai

*The Institute of Physical and Chemical Research (RIKEN), 2-1 Hirosawa, Wako, Saitama 351-01, Japan*

Issei Imamura and Fumiyuki Marumo

*Department of Earth Science, College of Humanities and Science, Nihon University,  
3-25-40 Sakurajosui, Setagaya-ku, Tokyo 156, Japan*

Ryochi Suzuki and Hiroyuki Ozaki

*Department of Material Systems Engineering, Tokyo University of Agriculture and Technology, Koganei, Tokyo 184, Japan*

Masaru Aoki and Shigeru Masuda

*Department of Chemistry, Graduate School of Arts and Sciences, The University of Tokyo, Komaba, Meguro-ku, Tokyo 153, Japan*

Misako Aida

*Biophysics Division, National Cancer Center Research Institute, 5-1-1 Tsukiji, Chuo-ku, Tokyo 104, Japan  
(Received 25 April 1997)*

Evidence for a molecule-substrate hybridized state near the Fermi level  $E_F$  is presented for Pd(110)- $c(4 \times 2)$ -benzene. Observed images of adsorbed benzene near  $E_F$  by scanning tunneling microscopy consist of two elongated protrusions separated by a single nodal depression with  $C_2$  symmetry. The existence of a benzene derived state near  $E_F$  is also observed by metastable atom electron spectroscopy, and it is assigned to the antibonding states between the  $1e_{1g}$  molecular orbital of benzene and the Pd  $4d$  orbitals by *ab initio* molecular orbital calculations. [S0031-9007(97)04504-3]

PACS numbers: 68.35.Bs, 82.65.My

Scanning tunneling microscopy (STM) images of adsorbed molecules on solid surfaces could provide valuable information on the adsorption sites, the orientation of individual molecules with respect to the substrate lattice, the periodicity of ordered molecular structures as well as defects and domains [1]. The observed internal structures are not directly related to the position of atoms, but to the electronic structure of adsorbed molecules and surfaces. It is known that the local density of states (LDOS) near the Fermi level  $E_F$  has a significant contribution to STM images [2–4]. In addition, observed STM images reflect the symmetry of both adsorption sites and molecular orbitals; in particular, the shape of the orbitals is of great importance [5]. Thus, in order to identify or discriminate among adsorbed species, the origin of observed STM images, i.e., the LDOS near  $E_F$  should be thoroughly characterized.

Adsorbed benzene on transition metal surfaces has been studied by both the STM experiments [6–9] and theoretical calculations [5,10,11]. Ohtani *et al.* have first reported high-resolution STM images of benzene molecules in the Rh(111)- $(3 \times 3)$  ( $C_6H_6 + 2CO$ ) surface [6]. Their STM images show individual benzene molecules as three-fold ringlike features, which reflects the fact that the benzene molecules adsorb at hcp-type threefold hollow sites on Rh(111) [12]. Weiss and Eigler [7] have reported three different STM images of isolated benzene molecules on Pt(111) at 4 K, which are ascribed to benzene molecules on three different adsorption sites [5]. According to ultraviolet

photoemission spectroscopy (UPS) [13–17] and inverse photoemission spectroscopy (IPES) [18,19] measurements of adsorbed benzene on transition metal surfaces, the highest occupied molecular orbital (HOMO) derived states are observed at 4–5 eV below  $E_F$  and the lowest unoccupied molecular orbital (LUMO) related states are observed at 2–3 eV above  $E_F$ , respectively. It has been supposed that these states have additional LDOS near  $E_F$  owing to resonance broadening [3,20], and thus STM can probe benzene molecules as a protrusion. However, the local electronic structure of adsorbed benzene on transition metal surfaces near  $E_F$  is not fully understood yet, because conventional UPS and IPES observe several surface layers and adsorbates, and thus it is difficult to probe the LDOS above the surface selectively.

In this Letter, we will elucidate the origin of internal structures of STM images in Pd(110)- $c(4 \times 2)$ -benzene. In order to probe the LDOS above the surface, we have applied metastable atom electron spectroscopy (MAES) using a  $He^*$  ( $2^3S$ ) beam. Based on *ab initio* MO calculations, benzene derived states that are observed near  $E_F$  by MAES are assigned to antibonding states formed through a combination of the benzene  $1e_{1g}$  orbital (HOMO) and the Pd  $4d$  band. The density profile of these states resembles the STM images of Pd(110)- $c(4 \times 2)$ -benzene.

Experiments were performed in an ultrahigh vacuum system ( $<1 \times 10^{-10}$  Torr) equipped with a three-grid retarding field analyzer for LEED and Auger electron

spectroscopy (AES), a quadrupole mass spectrometer, and a Beetle-type STM [9,21]. The Pd(110) surface was cleaned by repeated Ar-ion sputtering, annealing, oxidation, and flashing ( $\sim 1100$  K) cycles. The attainment of a clean Pd(110) ( $1 \times 1$ ) surface was confirmed by AES, LEED, and STM. We used an electrochemically etched tungsten tip or an electrochemically etched Pt-Ir tip. In the present study, all STM images were observed at room temperature. Experimental details of the He I UPS and He\* ( $2^3S$ ) MAES measurements were reported elsewhere [22].

We prepared the  $c(4 \times 2)$ -benzene on Pd(110) by dosing gaseous benzene onto Pd(110) at room temperature and annealing to  $\sim 320$  K. Well-ordered  $c(4 \times 2)$  structures were confirmed by both LEED and STM, and thermal decomposition does not occur under these conditions [23]. From our previous STM study, benzene molecules adsorb on the hollow sites of Pd(110) [9].

Figure 1 shows a series of STM images of the same area as a function of tip bias voltage ( $V_t$ ) from +1 to  $-1$  V with a constant tunneling current ( $I_t = 0.6$  nA). There are defects at the top of each image. At higher bias voltages ( $|V_t| \geq 1$  V) (Fig. 1), each adsorbed benzene molecule shows approximately a round shape. At low tip bias ( $|V_t| \leq 0.5$  V), the molecular image starts to split into two parts. It is clearly seen that a single nodelike depression exists for a molecule with its direction  $50^\circ$ – $60^\circ$  from  $[1\bar{1}0]$ . Note that the direction of the depression and the shape of protrusions change slightly as a function of tip bias voltage.

In order to confirm that these are intrinsic features of the system and not tip-induced effects, control experiments have been performed as follows. First, the scanning direction of the tip against the surface was varied. Second, we have used both tungsten and Pt-Ir tips. Al-

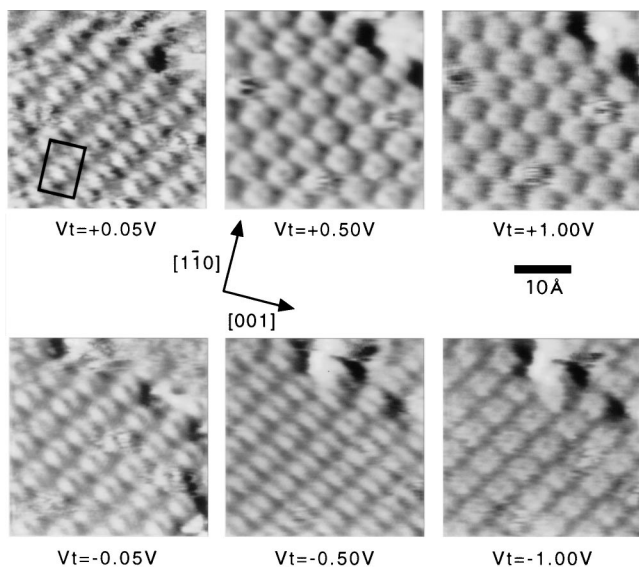


FIG. 1. A series of STM images of the identical area as a function of the tip bias voltage ( $V_t$ ) between +1 to  $-1$  V ( $I_t = 0.6$  nA). Positive (negative) tip bias corresponds to occupied (unoccupied) states of the system, respectively.

though slight differences in STM images were observed with different tips, which might be attributed to tip effects, a molecular image at a low bias voltage consisting of two elongated protrusions separated by a single depression with its direction  $50^\circ$ – $60^\circ$  from  $[1\bar{1}0]$  was observed in each case.

According to the UPS study by Netzer *et al.* [17], it has been proposed that the molecular plane of adsorbed benzene in the  $c(4 \times 2)$  structure is slightly tilted ( $\sim 10^\circ$ – $20^\circ$ ) from the surface in the  $[001]$  direction, keeping a vertex of benzene hexagon towards  $[1\bar{1}0]$ . While the symmetry of an isolated benzene molecule is  $D_{6h}$ , the symmetry of a tilted benzene on Pd(110), as proposed by Netzer *et al.* [17], cannot be higher than  $C_s$ . Vibrational spectra of this system indicate that the symmetry of adsorbed benzene is  $C_s$  or lower [23]. However, the present STM observation of internal structure for  $c(4 \times 2)$ -benzene on Pd(110) clearly shows  $C_2$  (or lower) symmetry at low bias voltages. Moreover, little indication for the “tilt” of adsorbed benzene was observed. These results are interpreted to indicate that the benzene molecules in the  $c(4 \times 2)$  structure may be azimuthally rotated from a symmetric orientation [15,16], which will be discussed later.

In order to clarify the electronic states of chemisorbed benzene near  $E_F$ , we have measured MAES spectra of the clean Pd(110) and  $c(4 \times 2)$ -benzene surfaces at room temperature. The data using a thermal He\* ( $2^3S$ , 19.8 eV) beam are shown in Fig. 2. For comparison the He I (21.2 eV) photoemission spectrum of the  $c(4 \times 2)$ -benzene is also shown. The bands A–E are assigned to the benzene derived  $1e_{1g}$ ,  $2e_{2g} + 1a_{2u}$ ,  $2e_{1u} + 1b_{2u} + 1b_{1u}$ ,  $2a_{1g}$ , and  $1e_{2g}$  states, respectively [17]. As compared with the UP spectrum of a benzene multilayer, the  $1e_{1g}$  (HOMO) peak of  $c(4 \times 2)$ -benzene is shifted by  $\sim 1$  eV to higher binding energy, because hybridization between the HOMO and the  $d$  orbitals of the substrate takes place. Note that only the shift of the  $1e_{1g}$  derived peak to higher binding energy has been observed in previous UPS studies [13–17], but the corresponding antibonding hybridized states have not been observed experimentally so far. This is due to strong photoemission from the substrate  $d$  bands near  $E_F$ , which makes it difficult to observe the antibonding state.

This difficulty can be overcome by means of MAES, since metastable atoms as the excitation source do not penetrate into the bulk and the electron emission spectrum selectively provides information on the outermost surface layer [24,25]. On the clean surface, the He\* ( $2^3S$ ) atoms deexcite predominantly via resonance ionization (RI) followed by Auger neutralization (AN) and give a broad feature reflecting the self-convolution of the local density of states [25]. The RI + AN process is still dominant on the  $c(4 \times 2)$ -benzene surface, but some of the He\* ( $2^3S$ ) atoms decay through Penning ionization (PI) to yield the same final states as in photoemission [25]. In fact, the threshold of electron emission in the He\* spectrum

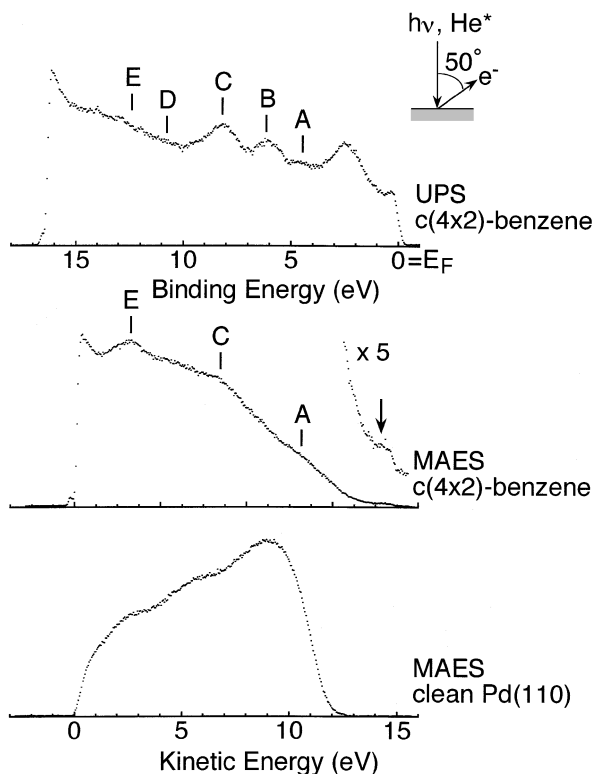


FIG. 2. Metastable atom electron spectra of the clean Pd(110) and  $c(4 \times 2)$ -benzene surfaces using  $\text{He}^*$  ( $2^3S$ , 19.8 eV) atoms. Photoemission spectrum of the  $c(4 \times 2)$ -benzene surface using He I (21.2 eV) resonance line is also shown. To facilitate comparison, the energy scale for the He I spectrum is shifted to that for the  $\text{He}^*$  spectra by the difference in the excitation energies,  $21.2 - 19.8 = 1.4$  eV.

coincides with that in the He I spectrum once the difference in the excitation energy is taken into account. Further, some of the benzene-derived bands indicated by vertical bars appear in the  $\text{He}^*$  spectrum [26]. Since the rate of PI is determined essentially by the overlap between the He  $1s$  orbital and surface orbitals that extend into the vacuum, a weak peak near  $E_F$  in the  $\text{He}^*$  spectrum indicated by the arrow is also related to the chemisorbed benzene.

In order to understand the nature of the chemical bonding in adsorbed benzene on Pd(110), we have performed *ab initio* MO calculations for the benzene-Pd(110) model using HONDO 95.3 [27]. The double-zeta quality basis sets augmented with polarization functions were used with compact effective potentials [28,29]. A cluster of five Pd atoms, which are composed of a rectangle ( $2.75 \times 3.89 \text{ \AA}$ ) of four Pd atoms and one additional Pd atom,  $1.385 \text{ \AA}$  below the rectangle at the center, was taken as a model of the Pd(110) surface. All the interaction energies were calculated at the MP2 level [30] by varying the distance  $R$  and azimuthal angle  $\theta$  between the Pd rectangular plane and the benzene molecule. The geometries of benzene and the Pd cluster were kept fixed. Details of the calculations will be reported elsewhere [31].

Figure 3(a) shows the energy diagram of free benzene and the benzene-five Pd atom model. Here, the distance

( $R$ ) between the molecular plane of benzene and the first Pd layer is  $1.95 \text{ \AA}$ , and the corner of the benzene molecule is rotated by  $\theta = 10^\circ$  from the  $[1\bar{1}0]$  direction. (Note that the  $10^\circ$  rotation is not the result of the energy optimization.) Since the molecular orbitals below  $2e_{2g}$  do not strongly interact with the Pd  $4d$  orbitals, we focused our attention on the interaction between the  $1e_{1g}$  and Pd  $4d$  orbitals. The  $1e_{1g}$  derived peak at  $\sim 4.5$  eV below  $E_F$  which has been observed by UPS is attributed to the bonding states just below the Pd  $4d$  states in Fig. 3(a). On the other hand, the new peak near  $E_F$  observed in the MAES results of Fig. 2 is assigned to the upper hybridized (antibonding) states.

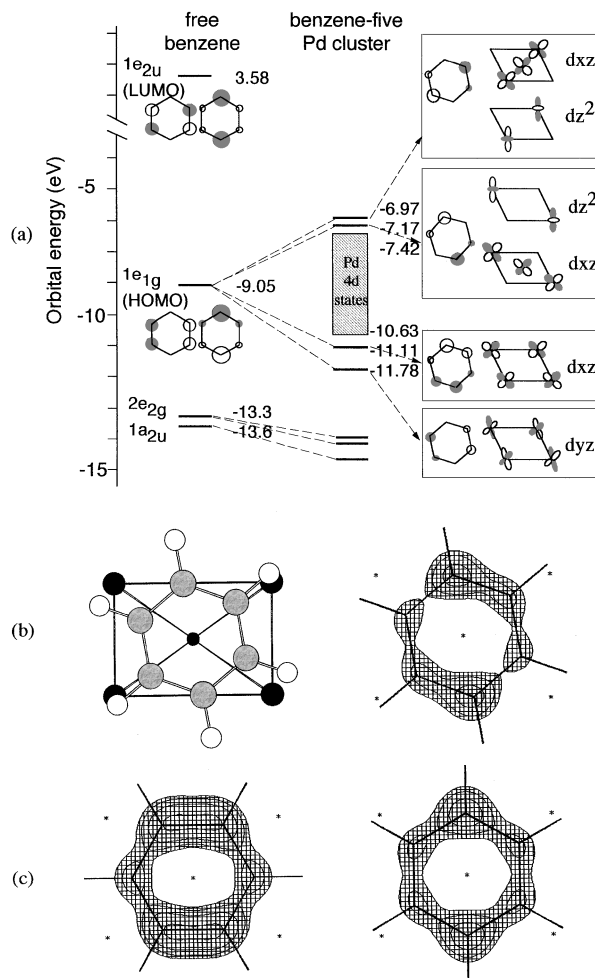


FIG. 3. (a) Orbital diagrams of free benzene and benzene-five Pd cluster system. In the cluster system, the benzene molecule is rotated by  $10^\circ$ . Note that the rotation brings about the specific interactions between benzene  $\pi$  orbitals and Pd  $d$  orbitals. (b) Density profiles above the benzene plane of the benzene-five Pd cluster system ( $C_2$  symmetry) in which the benzene molecule is rotated by  $10^\circ$ . The electron densities of the upper two antibonding states are overlaid. The geometry of calculated cluster system is also shown. (c) Density profiles above the benzene planes of the symmetrically adsorbed ( $C_{2v}$  symmetry) benzene-five Pd cluster systems. The electron densities of the upper two antibonding states are overlaid in each system.

We should note that the MO picture for chemisorption may overestimate the roles of the metal  $d$  orbitals because it does not include the extended structure of  $s$  and  $p$  bands which induces the broadening of adsorbate discrete states. As another limiting model, an adsorbate-derived resonance picture predicts that the level of the adsorbate HOMO or LUMO is resonantly broadened and somewhat shifted by the interaction with the metal bands [3,20]. However, recent experimental [32,33] and theoretical [34] studies have revealed that hybridization (=mixing) takes place in chemisorption on transition metals. Of course, a hybridized state is broadened due to the interaction with the metal bands.

Figures 3(b) and 3(c) show the local density profiles of the upper two states of azimuthally "rotated" ( $C_2$ ) benzene and symmetrically adsorbed ( $C_{2v}$ ) benzene on five Pd atoms, respectively. It is clearly seen in Fig. 3(b) that there are two elongated parts separated by a single node perpendicular to the molecular plane. On the other hand, in Fig. 3(c), the electron density uniformly exists over the molecule. Thus, the calculated electron density distributions for the  $C_{2v}$  and  $C_2$  models are qualitatively different in that only the  $C_2$  model predicts a nodal feature. Furthermore, because of the  $10^\circ$  azimuthal rotation, the node predicted for the  $C_2$  model is oriented  $\sim 45^\circ$  from  $[1\bar{1}0]$ . Therefore, we conclude that the observed internal structure at low  $V_t$  (near  $E_F$ ) in Fig. 1 predominantly reflects the antibonding hybridized states formed between the benzene HOMO and the Pd  $4d$  orbitals.

Azimuthally rotated adsorbed benzene molecules have been observed for densely packed benzene molecules on transition metal surfaces [15,16]. From detailed UPS measurements of  $c(4 \times 2)$ -benzene on Ni(110), Steinrück *et al.* [15] proposed that the molecule adsorbs as a flat-lying species, but it is azimuthally rotated. Azimuthal rotation of densely adsorbed flat-lying benzene takes place in order to decrease the repulsive interaction between benzene molecules [15,16,35].

In conclusion, the molecular images of  $c(4 \times 2)$  benzene molecules on Pd(110) by STM consist of two elongated protrusions separated by a single nodal depression with  $C_2$  symmetry. MAES has successfully probed a benzene-derived band near  $E_F$ . The origin of the observed STM images is ascribed to the antibonding states hybridized between the benzene  $1e_{1g}$  (HOMO) and the Pd  $4d$  orbitals by *ab initio* MO calculations.

The numerical calculations were carried out on the IBM/RS6000 Powerstations at the National Cancer Center Research Institute and on the SP2 at the computer center of the Institute for Molecular Science. The present work has been partly defrayed by the Grant-in-Aid on Priority-Area-Research on "Extreme environment catalysis" from the Ministry of Education, Science, Sports, and Culture of Japan (07242271), the JSPS Research for the

Future Program (96P00205), and the CREST program by JST.

---

\*Present address: The Institute for Solid State Physics, The University of Tokyo, 7-22-1 Roppongi, Minato-ku, Tokyo 106 Japan.

- [1] R. Wiesendanger, *Scanning Probe Microscopy and Spectroscopy* (Cambridge University Press, Cambridge, 1994).
- [2] J. Tersoff and D. R. Hamann, *Phys. Rev. B* **31**, 805 (1985).
- [3] N. D. Lang, in *Scanning Tunneling Microscopy III*, edited by R. Wiesendanger and H. J. Güntherodt (Springer-Verlag, Berlin, 1993), p. 7.
- [4] M. Tsukada *et al.*, *Surf. Sci. Rep.* **13**, 265 (1991).
- [5] P. Sautet and M. L. Bocquet, *Phys. Rev. B* **53**, 4910 (1996).
- [6] H. Ohtani *et al.*, *Phys. Rev. Lett.* **60**, 2398 (1988).
- [7] P. S. Weiss and D. M. Eigler, *Phys. Rev. Lett.* **71**, 3139 (1993).
- [8] S. J. Stranick *et al.*, *Surf. Sci.* **338**, 41 (1995).
- [9] J. Yoshinobu, H. Tanaka, T. Kawai, and M. Kawai, *Phys. Rev. B* **53**, 7492 (1996).
- [10] P. Sautet and C. Joachim, *Chem. Phys. Lett.* **185**, 23 (1991).
- [11] N. Isshiki *et al.*, *Appl. Surf. Sci.* **67**, 241 (1993).
- [12] R. F. Lin *et al.*, *Acta Crystallogr. Sect. B* **43**, 368 (1987).
- [13] J. E. Demuth and D. E. Eastman, *Phys. Rev. Lett.* **32**, 1123 (1974).
- [14] P. Hofmann *et al.*, *Surf. Sci.* **105**, L260 (1981).
- [15] W. Huber, M. Weinelt, P. Zebisch, and H.-P. Steinrück, *Surf. Sci.* **253**, 72 (1991).
- [16] M. Neuber *et al.*, *J. Phys. Chem.* **99**, 9160 (1995).
- [17] F. P. Netzer *et al.*, *Phys. Rev. B* **37**, 10399 (1988).
- [18] K. H. Frank *et al.*, *J. Chem. Phys.* **89**, 7569 (1988).
- [19] F. P. Netzer and K. H. Frank, *Phys. Rev. B* **40**, 5223 (1989).
- [20] B. Gumhalter, K. Wandelt, and Ph. Avouris, *Phys. Rev. B* **37**, 8048 (1988).
- [21] K. Besocke, *Surf. Sci.* **181**, 145 (1987).
- [22] H. Ishii, S. Masuda, and Y. Harada, *Surf. Sci.* **239**, 222 (1990).
- [23] M. Fujisawa *et al.*, *J. Phys. Chem.* **95**, 7415 (1991).
- [24] Y. Harada, S. Masuda, and H. Ozaki, *Chem. Rev.* (to be published).
- [25] W. Sesselmann *et al.*, *Surf. Sci.* **146**, 17 (1984).
- [26] S. Masuda, M. Aoyama, K. Ohno, and Y. Harada, *Phys. Rev. Lett.* **65**, 3257 (1990).
- [27] M. Dupuis, A. Marquez, and E. R. Davidson, HONDO 95.3 from CHEM-Station, IBM Corporation (1995).
- [28] W. J. Stevens *et al.*, *J. Chem. Phys.* **81**, 6026 (1984).
- [29] W. J. Stevens *et al.*, *Can. J. Chem.* **70**, 612 (1992).
- [30] C. Moller and M. S. Plesset, *Phys. Rev.* **46**, 618 (1934).
- [31] M. Aida (to be published).
- [32] A. Nilsson *et al.*, *Phys. Rev. B* **51**, 10224 (1995).
- [33] A. Nilsson *et al.*, *Phys. Rev. Lett.* **78**, 2847 (1997).
- [34] J. J. Mortensen, Y. Morikawa, B. Hammer, and J. K. Nørskov, *Z. Phys. Chem.* **198**, 113 (1997).
- [35] T. Fox and N. Rösch, *Surf. Sci.* **256**, 159 (1991).